Inorg. Chem. **2004**, *43*, 8169–8175

Structural, Magnetic, and Transport Properties of the $SrTi_{1-x}Co_xO_{3-\delta}$ Perovskite ($0 \leq x \leq 0.9$)

S. Malo* and A. Maignan

Laboratoire CRISMAT, UMR 6508 CNRS ISMRA, 6 bd Maréchal Juin, 14050 Caen Cedex 4, France

Received July 20, 2004

The series of the $SrTi_{1-x}Co_xO_{3-\delta}$ polycrystalline samples has been prepared via solid-state reaction in air. The structural study shows that a solid solution exists for all compositions, such as $0 \leq x \leq 0.9$, which discards the presence of ferromagnetic and metallic cobalt clusters for the low level of cobalt substitution. The existence of systematic extra peaks on the electron diffraction patterns for $x > 0.5$ indicates that the oxygen vacancy ordering is responsible for the superstructures ($2a_p \times 2a_p \times 4a_p$, where the subscript "p" refers to the perovskite subcell). The oxygen nonstoichiometry is confirmed by thermogravimetric analysis. The magnetic properties reveal a maximum in the magnetic moment per mole of cobalt for $x \approx 0.10$. However, the clear lack of strong ferromagnetism does not suggest that a diluted magnetic semiconductor (DMS)-type behavior is induced in $SrTiO_3$ as Co is substituted for Ti. The transport properties along the $SrTi_{1-x}Co_xO_{3-\delta}$ line are explained by considering the substitution of a Co^{3+}/Co^{4+} mixed valency, which decreases the room-temperature resistivity by at least 5 orders of magnitude as one goes from $SrTi_{0.9}Co_{0.1}O_{3-\delta}$ to $SrTi_{0.1}Co_{0.9}O_{3-\delta}$.

Introduction

There has been recent interest in oxide-diluted magnetic semiconductor (DMS) material, because the use of the spin electron in addition to the host property has potential applications in spintronics. In particular, the report of room-temperature ferromagnetism in several oxides, such as cobalt-doped anatase TiO_2[1] and cobalt-doped wurtzite,[2] is very promising. Nonetheless, the origin of this ferromagnetism is still an open question, because the presence of metallic ferromagnetic cobalt nanoclusters, which are responsible for these interesting properties, is not easy to detect in thin films. More recently, Co substitutions for Ti have been attempted in thin films of the perovskite titanates $SrTiO_3$[3] and $La_{0.5}Sr_{0.5}TiO_3$,[4] yielding contradicting results, because ferromagnetism is reported for the latter but not for the former.

To check for the ability of Co to be substituted for Ti, the $SrTi_{1-x}Co_xO_{3-\delta}$ series has been studied by preparing bulk samples in air. The end members, $SrTiO_3$ ($x = 0$) and $SrCoO_3$, are a band insulator[5,6] and a ferromagnetic metal,[7] respectively, and the study of this line is not only interesting on the titanium-rich side for DMS properties but also for the cobalt-rich side (to study the ferromagnetism dilution by Ti^{4+} cations). In the following, we report on the electrical (resistivity) and magnetic properties of air-prepared $SrTi_{1-x}Co_xO_{3-\delta}$ samples. The structural study performed by combining X-ray diffractometry (XRD) and electron diffraction reveals the existence of a superstructure for $x \geq 0.5$, which is attributed to the oxygen nonstoichiometry. Although strong ferromagnetism is not observed for the compositions that contain a small amount of cobalt, a clear maximum in the cobalt magnetic moment is revealed for $x \approx 0.10$.

Experimental Section

The samples were prepared in air by mixing $SrCO_3$, TiO_2, and Co_3O_4 precursors in stoichiometric amounts according to the formula $SrTi_{1-x}Co_xO_3$. After a decarbonatation at 1000 °C, the

* Author to whom correspondence should be addressed. Phone: (33)2-31-45-26-10. Fax: (33)2-31-95-16-00. E-mail address: sylvie.malo@ensicaen.fr.

(1) Matsumoto, Y.; Murakami, M.; Shono, T.; Hasegawa, T.; Fukumura, T.; Kawasaki, M.; Ahmet, P.; Chikyow, T.; Koshihara, S.; Koinuma, H. *Science* **2001**, *291*, 854.
(2) Ueda, K.; Tabata, H.; Kawai, T. *Appl. Phys. Lett.* **2001**, *79*, 988.
(3) Matsumoto, Y.; Takahashi, R.; Murakami, M.; Koida, T.; Fan, X. J.; Hasegawa, T.; Fukumura, T.; Kawasaki, M.; Koshihara, S. Y.; Koinuma, H. *Jpn. J. Appl. Phys., Part 2* **2001**, *40*, L1204.
(4) Dietl, T.; Ohno, H.; Matsukura, F.; Cibert, J.; Ferrand, D. *Science* **2000**, *287*, 1019.
(5) Zhao, Y. G.; Shinde, S. R.; Ogale, S. B.; Higgins, J.; Choudhary, R. J.; Kulkarni, V. N.; Greene, R. L.; Venkatesan, T.; Lofland, S. E.; Lanci, C.; Buban, J. P.; Browning, N. D.; Das Sarma, S.; Millis, A. J. *Appl. Phys. Lett.* **2003**, *83*, 2199.
(6) Fabricius, G.; Peltzer y Blanca, E. L.; Rodriguez, C. O.; Ayala, A. P.; de la Presa, P.; Lopez García, A. *Phys. Rev. B* **1997**, *55*, 164.
(7) Okuda, T.; Nakanishi, K.; Miyasaka, S.; Tokura, Y. *Phys. Rev. B* **2001**, *63*, 113104.

10.1021/ic0490371 CCC: $27.50
Published on Web 11/06/2004

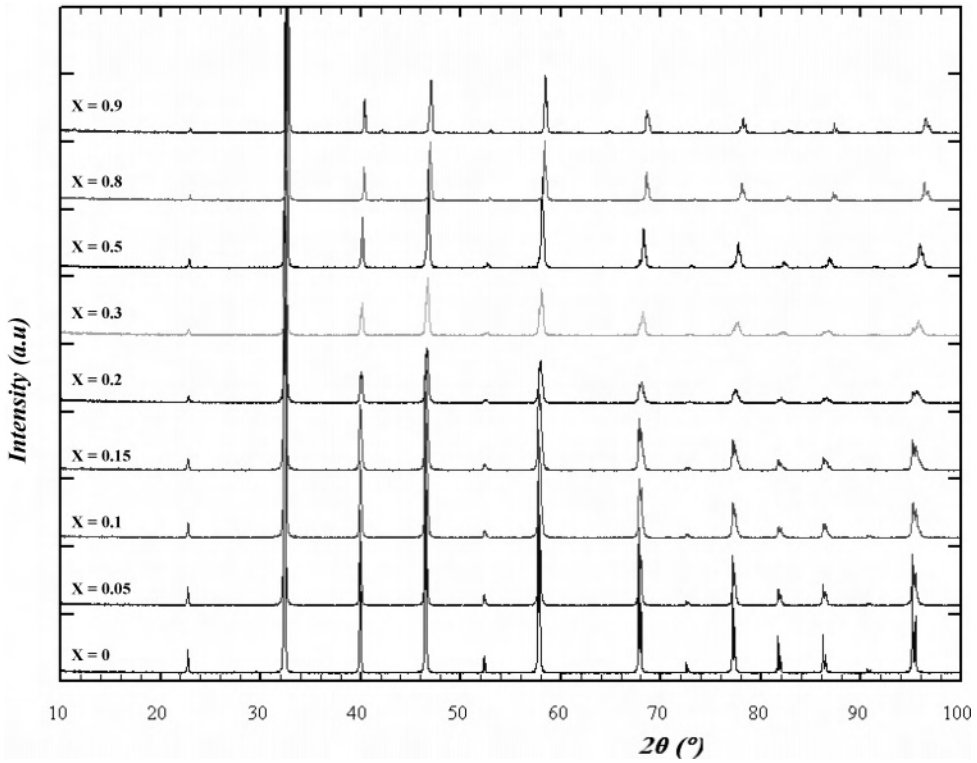

Figure 1. Powder X-ray diffraction (PXRD) data for $SrTi_{1-x}Co_xO_{3-\delta}$ ($0 \leq x \leq 0.9$).

powders were pressed in bars (~2 mm × 2 mm × 10 mm) and heated to 1100 °C at a rate of 2°C/min, held at this temperature for 12 h, and furnace-cooled to room temperature.

The samples were characterized by powder X-ray diffraction (PXRD) at room temperature using a Philips diffractometer, working with Cu Kα radiation in the 2θ range of 10°−100° with a step size of 0.02°. The PXRD data were analyzed using the Rietveld method (through application of the FULLPROF Program).[8]

The samples for transmission electron microscopy (TEM) analysis were crushed in alcohol, and the small flakes were deposited on a holey carbon film that was supported by a copper grid. The electron diffraction (ED) study was performed, at room temperature, on a JEOL model 200 CX electron microscope that had been fitted with an eucentric goniometer (±60°) and equipped with an energy-dispersive spectroscopy (EDS) analyzer.

The oxygen content was determined using the thermogravimetric hydrogen reduction method (Ar/10% H_2) on a Setaram model TAG92 microbalance.

The resistivity of the compounds has been measured by the four-probe technique on bars. Indium electrical contacts were deposited using ultrasonic waves. Measurements were made during cooling from 400 K to 5 K. The Seebeck coefficient (S) was measured by a steady-state method. Temperature (or magnetic-field)-dependent magnetization data were collected using a SQUID magnetometer. For the temperature-dependent data, the measurements were recorded upon warming (zero-field-cooling (zfc) and field-cooling (fc) processes).

Results

Structural Characterizations. The quality of the samples was first checked by powder X-ray diffraction (PXRD). Regardless of the value of x, the PXRD patterns were similar to that of the original $SrTiO_{3-\delta}$ (i.e., $x = 0$) sample, which indicates that they crystallized in the same type of structure (Figure 1). The small systematic shift observed in the peak positions as x increases is in agreement with the progressive Co substitution for the Ti. This cationic substitution was confirmed by EDS analyses that were performed on numerous crystallites of all the samples. The average cationic compositions of the samples determined experimentally are similar to the nominal values, within the experimental error. The structural model used for refining the PXRD was based on a $Pm\bar{3}m$ cell with a lattice parameter of $a \approx a_p \approx 3.85$ Å and a statistical distribution of the Ti and Co species on the B site. The data were refined using the Rietveld method, and the lattice parameters are reported in Table 1 with the reliability factors. The lattice parameter decreases as the cobalt content increases, following Vegard's law, as illustrated in Figure 2. This behavior is expected for a solid solution when the cationic substitution does not change the structure strongly.

Table 1. $SrTi_{1-x}Co_xO_{3-\delta}$: Lattice Parameters Refined with the Rietveld Method from X-ray Diffractometry at Room Temperature in the Space Group $Pm\bar{3}m$ and a Statistical Occupation of the B-site

x	a (Å)	χ^2	R_{Bragg}	R_F
0	3.9047(1)	4.33	4.12	2.84
0.05	3.9032(1)	2.79	4.44	3.77
0.1	3.8996(2)	2.79	6.25	4.63
0.15	3.8972(2)	3.57	5.05	3.74
0.2	3.8951(2)	1.55	3.92	2.96
0.3	3.8895(2)	2.77	5.30	3.73
0.5	3.88201	2.74	5.51	4.15
0.8	3.8678(2)	2.15	7.57	4.99
0.9	3.8637(2)	2.67	9.02	5.48

The electron diffraction (ED) study, performed at room temperature, shows that the reflections for the samples with

(8) Bezdicka, P.; Wattiaux, A.; Grenier, J. C.; Pouchard, M.; Hagermuller, P. *Z. Anorg. Allg. Chem.* **1993**, *619*, 7.

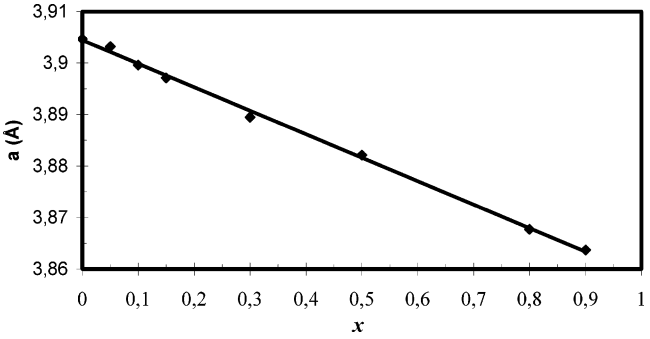

Figure 2. Evolution of the lattice parameters versus x in $SrTi_{1-x}Co_xO_{3-\delta}$.

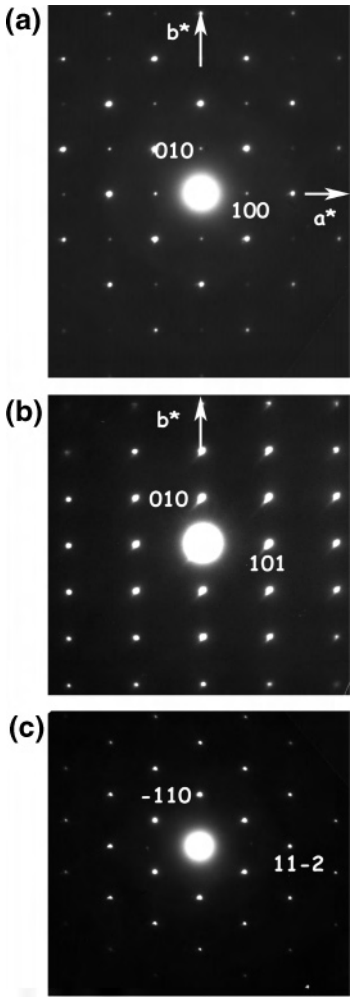

Figure 3. Electron diffraction patterns ((a) (001)*, (b) ($\bar{1}$01)*, and (c) (111)*) recorded on $SrTi_{0.7}Co_{0.3}O_{3-\delta}$.

$x \leq 0.5$ are characteristic of the perovskite structure. The cell is cubic with $a \approx a_p$ and no conditions are limiting the reflection, which is in agreement with the $Pm\bar{3}m$ space group. The (001), ($\bar{1}$01), and (111) ED patterns that have been recorded on $SrTi_{0.7}Co_{0.3}O_{3-\delta}$ are represented in Figure 3. When $x > 0.5$, extra reflections appear on the ED patterns. For x values just beyond 0.5, barely diffused extra reflections are observed along the [100] direction, as indicated by the small white arrows in Figure 4 for $SrTi_{0.43}Co_{0.57}O_{3-\delta}$ ($x = 0.57$). These extra reflections imply a doubling of the lattice parameter along at least one direction. These crystallites, which exhibit diffused reflections on the ED patterns, present

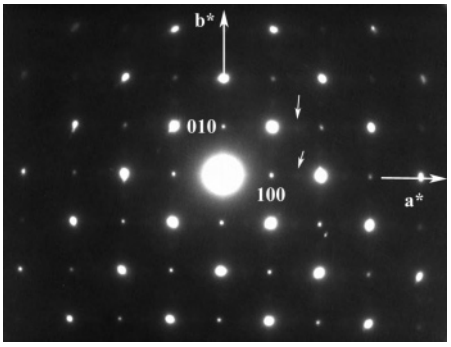

Figure 4. Electron diffraction pattern (along [001]) recorded on $SrTi_{0.43}Co_{0.57}O_{3-\delta}$; the small white arrows indicate diffuse extra reflections.

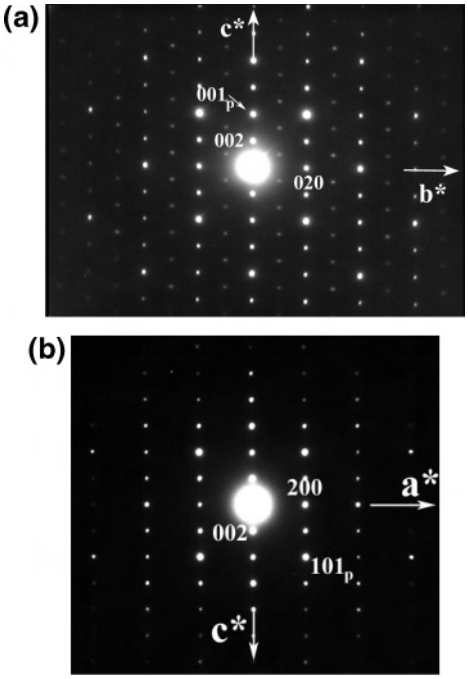

Figure 5. Electron diffraction patterns recorded on $SrTi_{0.1}Co_{0.9}O_{3-\delta}$ along the (a) [100] and (b) [010] directions; the white arrows indicate extra reflections due to twinned domains, and the subscript "p" corresponds to the indexation in the cubic perovskite subcell.

twinned domains. As x increases, these extra reflections become more and more intense and punctual. For $x = 0.9$, the reconstruction of the reciprocal space by tilting around crystallographic axes evidenced a supercell with $a \approx 2a_p$, $b \approx 2a_p$, and $c \approx 4a_p$, with the following conditions limiting the reflections: for hkl, $h + k + l = 2n$; for $h0l$, $l = 2n$; and for $hk0$, $k = 2n$, which are compatible with the space groups *Imcb or I2cb*. The (100)* and (010)* ED patterns are shown in Figure 5. Most of the ED patterns recorded for the cobalt-rich samples exhibit twinned domains, which makes determination of the cell ambiguous, because of the simple relationships between the lattice parameters. The ED pattern, on which the (010)* and (001)* planes overlap, illustrates this problem in Figure 6, where the small white arrows indicate the reflections that do not correspond to the (100)* plane. A quadrupling along one axis of the cubic perovskite cell had been already evidenced in cobaltite ($SrCo_{0.9}Sc_{0.1}O_{3-\delta}$),[9]

(9) Rodriguez-Carvajal, J.; Fullprof, Mai 2003 Version, LLB−CEA, Saclay, France.

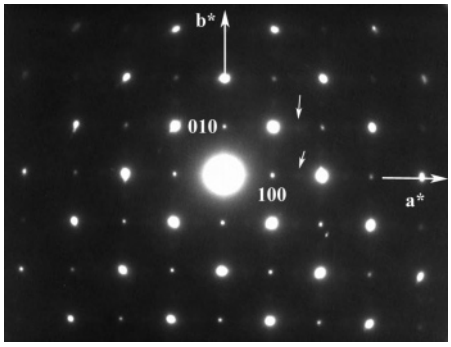

Figure 6. Electron diffraction pattern (along [100]) recorded on a crystallite $SrTi_{0.1}Co_{0.9}O_{3-\delta}$ exhibiting twinned domains; the small white arrows indicate extra reflections due to this twining.

which also contained 10% foreign cations on the B-site. However, for the latter, the ED study evidenced a primitive cell with the following parameters: $2a_p\sqrt{2} \times 2a_p\sqrt{2} \times 4a_p$. The difference in space groups could be linked to the different oxidation states of the foreign cations (trivalent and tetravalent for scandium and titanium, respectively), which imply different cobalt oxidation states and/or different oxygen contents. The thermogravimetric analysis (TGA) that was performed on the samples corresponding to $x = 0.05$, 0.1, 0.3, and 0.5 provides evidence that oxygen vacancies are created as soon as Co is substituted for Ti. For these samples ($SrTi_{1-x}Co_xO_{3-\delta}$), the oxygen deficiencies are observed to be $\delta \approx 0.04$, 0.08, 0.16, and 0.19 for $x = 0.05$, 0.1, 0.3, and 0.5, respectively. However, as previously mentioned, no long-range ordering has been observed in these samples, which suggests a random distribution of the oxygen vacancies. These results confirm the difficulty to synthesize fully oxidized perovskites with Co^{4+} cations under normal conditions.[9] It was impossible to determine the oxygen content for the cobalt-rich sample ($x = 0.9$) using either TGA (because of the incomplete reduction of cobalt) or redox titrations (because of the very low solubility of the sample).

For $SrTi_{0.1}Co_{0.9}O_{3-\delta}$, the I-type centering with a cell parameter such as $c = 4a_p$ (where a_p is the cell parameter of the primitive perovskite) is similar to that reported for several A-site-substituted strontium-based cobalt perovskites ($Ln_{1-y}Sr_yCoO_{3-\delta}$, where Ln = Sm−Yb (and Y) and $y \leq 0.9$, with the smaller y values being dependent on the lanthanide).[10−12] The origin of this $2a_p \times 2a_p \times 4a_p$ superstructure was explained by the existence of a coupled Ln/Sr and oxygen/vacancy ordering. The presence of only Sr^{2+} cations at the A-site of the perovskite in $SrTi_{0.1}Co_{0.9}O_{3-\delta}$ allows us to exclude the role of A-site cationic ordering; however, the mixed (Ti/Co) B-site occupancy could also be responsible for a cationic ordering on this site. A more-detailed study that combines high-resolution electron microscopy and neutron diffraction is now required for further examination of the ordering phenomena in this cobaltite.

(10) Maignan, A.; Pelloquin, D.; Flahaut, D.; Caignaert, V. *J. Solid State Chem.*, in press.
(11) James, M.; Cassidy, D.; Goossens, D. J.; Withers, R. L. *J. Solid State Chem.* **2004**, *177*, 1886.
(12) Withers, R. L.; James, M.; Goossens, D. J. *J. Solid State Chem.* **2003**, *174*, 198.

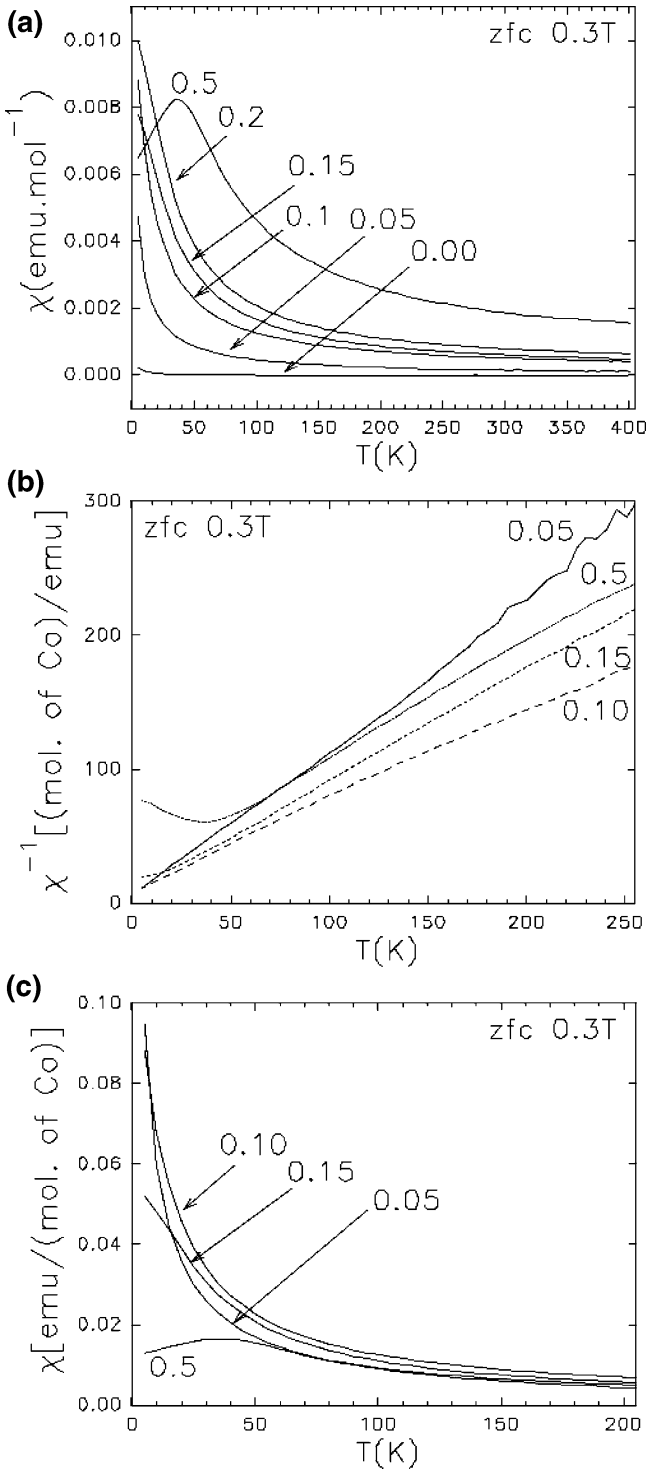

Figure 7. Temperature (T) dependence of (a) the magnetic susceptibility ($\chi = M/H$) and (b) the inverse magnetic susceptibility (χ^{-1}) for the $SrTi_{1-x}Co_xO_{3-\delta}$ series; the x values are labeled on the graph. Panel c shows the variation of $\chi(T)$ with χ, in units of emu per mole of cobalt.

Magnetic and Electrical Properties. The study of the magnetization (M), as a function of the temperature (T), for $SrTi_{1-x}Co_xO_{3-\delta}$ first reveals that these compounds do not exhibit a strong ferromagnetism, except on the cobalt-rich side. As shown in Figure 7a, the magnetic susceptibility (χ), which is calculated by dividing M by the magnetic field value, behaves almost the same as that for a paramagnet in a large T region (except for $x = 0.5$). This is confirmed by

Table 2. $SrTi_{1-x}Co_xO_{3-\delta}$: Effective Paramagnetic Moment (μ_{eff}) from the Paramagnetic Region of the $\chi^{-1}(T)$ Curves, Magnetization Values per Cobalt at 5 K and in a Magnetic Field of 5 T (M_{5K}), and the Resistivity Value at 300 K (ρ_{300K})

x	μ_{eff} per mole of Co	M_{5K}(5 T) (μ_B/mole of Co)	ρ_{300K} (Ω cm)
0.05	2.50	0.37	
0.10	3.67	0.59	1.2×10^3
0.20	3.25	0.34	2.0×10^2
0.50	not measured	0.11	
0.80	3.0	not measured	2.5×10^{-2}
0.90	not measured	not measured	6.0×10^{-3}

the linear $\chi^{-1}(T)$ curves found for all x values for $T < 70$ K (see Figure 7b). Furthermore, the extrapolation of these $\chi^{-1}(T)$ curves to zero leads to $\theta_p \approx 0$ K values, showing a lack of ferromagnetic interactions. Nevertheless, when the χ values in the paramagnetic regime are also plotted as $\chi(T)$ curves, relative to χ (in units of emu per mole of cobalt), they are not superimposed; instead, χ goes through a maximum for $SrTi_{0.9}Co_{0.1}O_{3-\delta}$ ($x = 0.1$) (see Figure 7c). This non-monotonic behavior of χ, relative to x, is also confirmed by the values of the effective paramagnetic moments extracted from the $\chi^{-1}(T)$ curves in the paramagnetic regime (Table 2). The μ_{eff} values go through a maximum for $x = 0.10$, whereas the value of μ_{eff} is almost constant for $x > 0.1$. To confirm this anomalous behavior, isothermal $M(H)$ data have been also collected at 5 K (Figure 8). Consistently, as the cobalt content decreases from 50% ($x = 0.5$) to 5% ($x = 0.05$), the highest M values under 5 T are observed to be attained for $x = 0.1$ and correspond to ~ 0.6 μ_B/mol of cobalt (see Figure 8a). These measurements also show the existence of a hysteresis in zero field (a remanent magnetization is observed in the enlargement shown in Figure 8b). Thus, if the magnetic behavior is almost paramagnetic at 5 K for $SrTi_{0.5}Co_{0.5}O_{3-\delta}$ (a linear $M(H)$ plot for $x = 0.5$), it clearly deviates from paramagnetism below $x < 0.5$, with rounded $M(H)$ curves, leading to the highest M values being observed for $x = 0.1$. The existence of an irreversible behavior is also confirmed by the comparison of $\chi(T)$ curves that correspond to the zero-field-cooling (zfc) and field-cooling (fc) modes (Figure 9), where the fc and zfc curves have a tendency to merge for $T \geq 30$ K and 50 K for $x = 0.1$ and $x = 0.5$, respectively. For all these cobalt contents, the magnetic behavior is not typical of a true paramagnet. The presence of some very small ferromagnetic clusters, diluted in the nonmagnetic matrix, leads to the superparamagnetic-like behavior, i.e., larger μ_{eff} values and rounded $M(H)$ curves are observed for the smallest x values. In contrast, the existence of a χ maximum on the zfc curve of $SrTi_{0.5}Co_{0.5}O_{3-\delta}$, together with the very low M_{5K}(5 T) value (~ 0.1 μ_B/mol of Co), suggests that the global magnetism is much weaker for large cobalt concentrations. If one considers the change in the μ_{eff} values, from 3.85 μ_B/mol of Co for $x = 0.1$ to 3.3 μ_B/mol of Co for $x = 0.5$, one can rule out a possible change toward a LS state for cobalt (for instance, low spin (LS) Co^{3+}, $S = 0$). It is more likely that, for a sufficiently high amount of cobalt, weak antiferromagnetic Co−O−Co interactions dominate. On the opposite side of the $SrTi_{1-x}Co_xO_{3-\delta}$ line, the samples exhibit much stronger ferromagnetic interactions, as shown in Figure 10, where a positive paramagnetic temperature ($\theta_P = 100$ K) is observed for $x = 0.9$. This behavior is consistent with the ferromagnetism of $SrCoO_3$ ($T_c \approx 290$ K).[7] In the present titanium compound, the presence of the nonmagnetic Ti^{4+} cation dilutes the Co^{4+}−O−Co^{4+} ferromagnetic interactions, whereas the existence of oxygen nonstoichiometry also breaks some

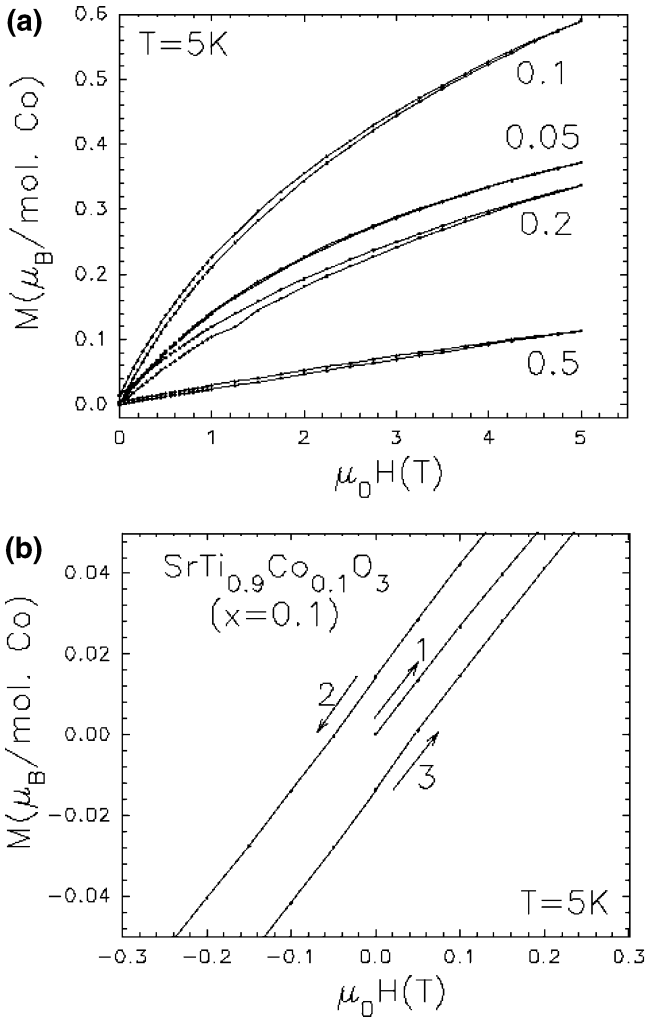

Figure 8. (a) Isothermal ($T = 5$ K) magnetic-field (H)-dependent magnetization (M) curves. Panel b shows an enlargement around $H = 0$ for the $SrTi_{0.9}Co_{0.1}O_{3-\delta}$ compound.

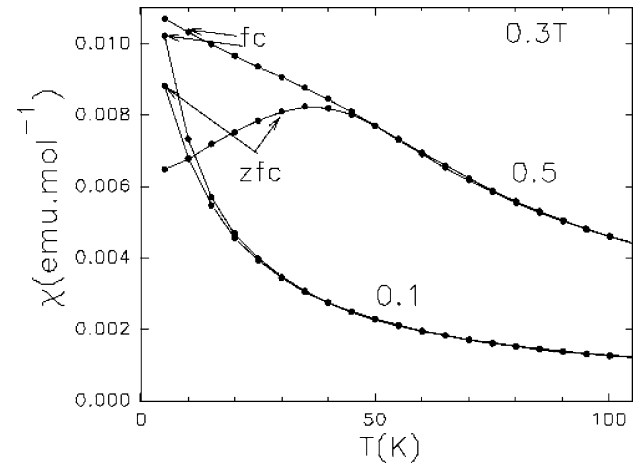

Figure 9. $\chi(T)$ curves collected in zero-field-cooling (zfc) and field-cooling (fc) modes for $SrTi_{0.9}Co_{0.1}O_{3-\delta}$ and $SrTi_{05}Co_{0.5}O_{3-\delta}$ ($\mu_0 H = 0.3$ T).

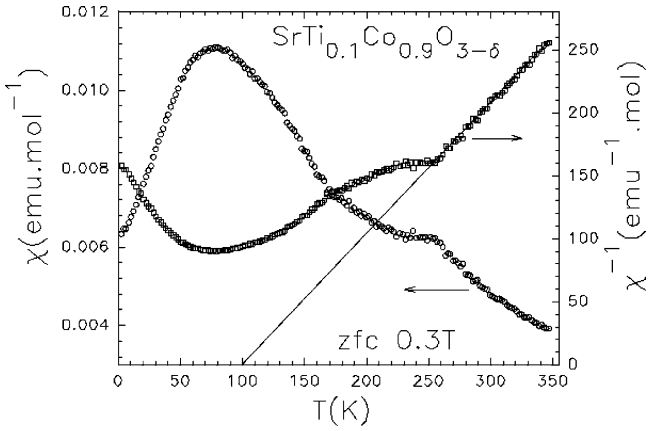

Figure 10. $\chi(T)$ and $\chi^{-1}(T)$ curves (left-hand axis and right-hand axis, respectively) for the $SrTi_{0.1}Co_{0.9}O_{3-\delta}$ compound; the line corresponds to the extrapolation of the paramagnetic regime to $\chi^{-1} = 0$, yielding $\theta_p = 100$ K.

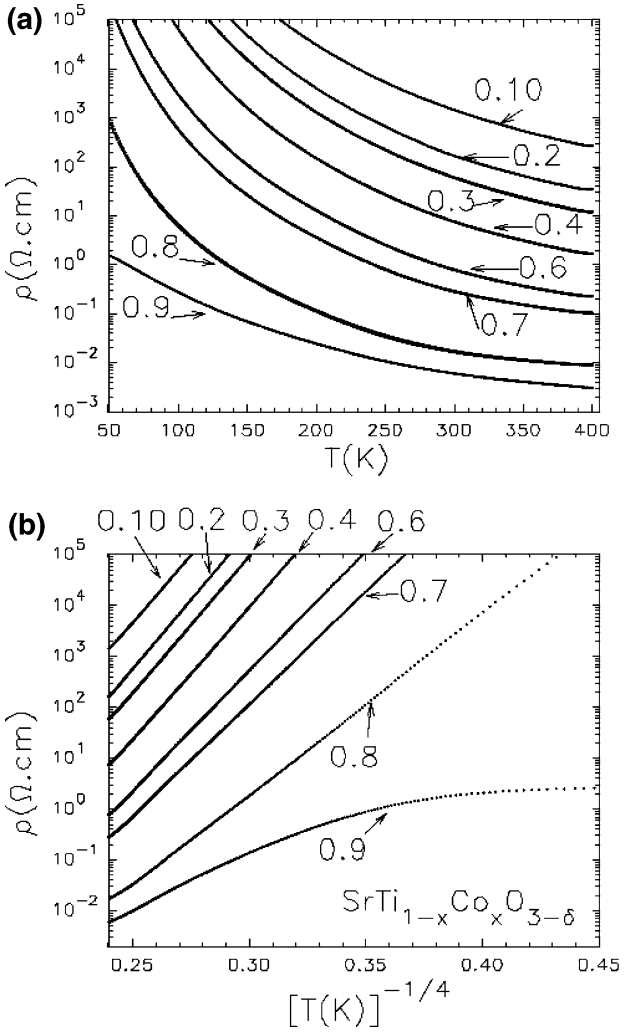

Figure 11. (a) Temperature (T) dependence of the electrical resistivity (ρ) for the $SrTi_{1-x}Co_xO_{3-\delta}$ compound; (b) plot of ρ as a function of $T^{-1/4}$.

ferromagnetic pathways and creates Co^{3+} species, which may or may not participate in the magnetism, depending on the Co^{3+} spin state.

Interestingly, the electrical transport behavior reflects the magnetism behavior in that series (Figure 11a). The room-temperature resistivity is the smallest on the cobalt-rich side, with typical ρ values of $\sim 10^{-3}-10^{-2}$ Ω cm for $x = 0.8-0.9$ in the $SrTi_{1-x}Co_xO_{3-\delta}$ series. This behavior is consistent with the metallicity that has been reported for $SrCoO_3$. As the cobalt content is decreased, the ρ_{300K} values continue to increase (see Table 1), reaching a maximum value for the lowest x values: $\rho_{300K} \approx 1$ kΩ cm for $x = 0.10$, and the ρ values exceed our experimental limits (resisitivity of $R < 10^6$ Ω) for $x = 0$ and $x = 0.05$. Thus, the existence of a larger magnetic moment for $x = 0.10$ has no direct consequence on the electrical behavior. Note also that the application of a magnetic field of 7 T does not modify the ρ values for all x values (such as $x \leq 0.8$), which agrees with the lack of strong ferromagnetism induced by the substitution of Co for Ti. Consequently, no significant magnetoresistance is evidenced on the isothermal $\rho(H)$ curves for T values below which the resistance sample is measurable ($R < 10^7$ Ω). It must also be emphasized that a semiconducting behavior with an activation energy is not found in these samples. In contrast, the variable range hopping (VRH) model for a three dimensional (3D) compound ($T^{-1/4}$) allows us to linearize the data, as shown in Figure 11b, where a clear change of conduction is revealed for $x = 0.9$. This VRH behavior, which is characteristic of the disordered systems, is consistent with the disorder that is induced by the mixed B-site occupation.

Discussion and Concluding Remarks

The present study of the $SrTi_{1-x}Co_xO_{3-\delta}$ series shows that the compounds crystallizing in the perovskite structure can be obtained by chemical reaction in air for x values in the range of $0 \leq x \leq 0.9$. Their structural study reveals several complex features with, in particular, the existence of superstructure peaks for all compositions, such as $x > 0.5$. By considering, on one hand, the stable tetravalent oxidation state for the Ti^{4+} cations under oxidizing conditions, and, on the other hand, the large oxygen pressure (6 GPa in the work of Kawasaki et al.[13]) required to prepare the oxygen-stoichiometric $SrCoO_3$ perovskite containing pure Co^{4+}, it is reasonable to assume that the oxidation state of cobalt is less than tetravalent in the $SrTi_{1-x}Co_xO_{3-\delta}$ series. This point is confirmed by the TGA results. From these data, the oxidation state of cobalt remains ~3, within the experimental error, at least for x values up to 0.5. Thus, the substitution is accompanied by the creation of oxygen vacancies. The ordering phenomena of the latter is responsible for the superstructure revealed by electron diffraction for the $x > 0.5$ compositions. To probe the nature of the carriers, the thermoelectric power (TEP) (the Seebeck effect, S) has been measured. A typical $S(T)$ curve is given in Figure 12 for $SrTi_{0.85}Co_{0.15}O_{3-\delta}$. In contrast to the TEP of pure $SrTiO_3$ and that of $Sr_{1-x}La_xTiO_3$ ($x \leq 0.10$; see ref 6), which clearly exhibits S_{300K} values of <0, which is characteristic of electron charge carriers, the present cobalt-substituted compound exhibits S values of >0, with $S_{300K} = 70$ μV/K, demonstrating that the transport mechanism is totally different. In the

(13) Istomin, S. Y.; Drozhzhin, O. A.; Svensson, G.; Antipov, E. V. *Solid State Sci.* **2004**, *6*, 539.

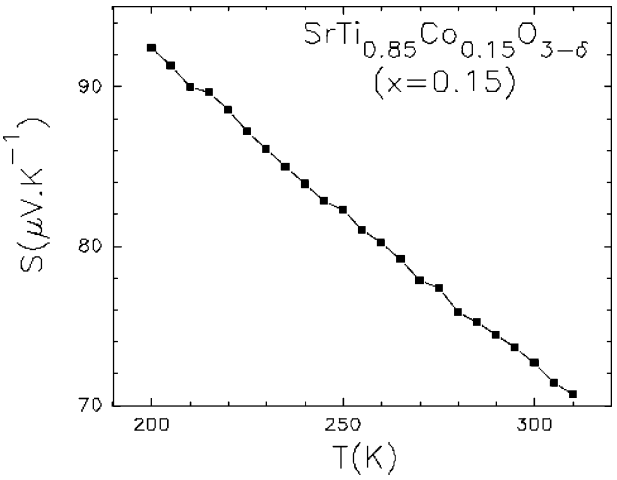

Figure 12. Temperature (T) dependence of the Seebeck coefficient (S) for $SrTi_{0.85}Co_{0.15}O_{3-\delta}$.

absence of a Ti^{3+}/Ti^{4+} mixed valency, the Co species are most probably responsible for the transport properties, because ρ monotonously decreases as the cobalt content increases. The hole character of the charge carriers in cobaltites, as in the $La_{1-x}Sr_xCoO_3$ perovskite, could explain these properties. Comparing the S_{300K} value for $SrTi_{0.85}Co_{0.15}O_{3-\delta}$ to those of the $La_{1-x}Sr_xCoO_3$ series,[14] the oxidation state of cobalt in the former would be between that of $La_{0.925}Sr_{0.075}CoO_3$ and that of $La_{0.85}Sr_{0.15}CoO_3$. Accordingly, the transport in the $SrTi_{1-x}Co_xO_{3-\delta}$ series could be explained by considering a Co^{3+}/Co^{4+} mixed valency, rather than the injection of an electron in the empty t_{2g} band of Ti^{4+}.

From the standpoint of physical properties, a clear lack of strong ferromagnetism in the diluted magnetic semiconductor (DMS) is evidenced in this series for the titanium-rich composition. However, the "enhancement" of the magnetism for the $SrTi_{0.9}Co_{0.1}O_{3-\delta}$ suggests that, for this composition, some local ferromagnetic Co−O−Co interactions are responsible for superparamagnetic behavior. For higher cobalt concentrations, the decrease of the magnetic moment per mole of cobalt as x increases in $SrTi_{1-x}Co_xO_{3-\delta}$ is supposed to be due to the existence of dominating antiferromagnetic Co−O−Co interactions.

The absence of ferromagnetism for small cobalt contents in $SrTiO_3$ demonstrates that when Co^{3+} cations are homogeneously substituted for Ti^{4+} cations, under the present oxidizing conditions, the solid solution cannot be considered for applications as DMS material in spintronics.

IC0490371

(14) Kawasaki, S.; Takano, M.; Takeda, Y. *J. Solid State Chem.* **1996**, *121*, 174.
(15) Señarís-Rodríguez, M. A.; Goodenough, J. B. *J. Solid State Chem.* **1995**, *118*, 323.